

Elsevier required licence: © <2022>. This manuscript version is made available under the CC-BY-NC-ND 4.0 license <http://creativecommons.org/licenses/by-nc-nd/4.0/>
The definitive publisher version is available online at
[\[https://www.sciencedirect.com/science/article/pii/S0301479722001621?via%3Dihub\]](https://www.sciencedirect.com/science/article/pii/S0301479722001621?via%3Dihub)

1 **Predicting soil erosion susceptibility associated with climate change**
2 **scenarios in the Central Highlands of Sri Lanka**

3 **Sumudu Senanayake^{1,2}, Biswajeet Pradhan^{1*,3,4,5}**

4 ¹ The Centre for Advanced Modelling and Geospatial Information Systems (CAMGIS), School of
5 Civil and Environmental Engineering, Faculty of Engineering and IT, University of Technology
6 Sydney, Sydney, 2007 NSW, Australia

7 ² Natural Resources Management Centre, Department of Agriculture, Peradeniya, 20400,
8 Sri Lanka.

9 ³ Department of Energy and Mineral Resources Engineering, Sejong University, Choongmu-gwan,
10 209 Neungdong-ro, Gwangjin-gu, Seoul 05006, Korea

11 ⁴ Center of Excellence for Climate Change Research, King Abdulaziz University, P. O. Box 80234,
12 Jeddah 21589, Saudi Arabia

13 ⁵ Earth Observation Center, Institute of Climate Change, University Kebangsaan Malaysia, 43600
14 UKM, Bangi, Selangor, Malaysia

15 * Correspondence: Biswajeet.Pradhan@uts.edu.au; or biswajeet24@gmail.com

16
17
18
19
20
21
22
23
24
25
26
27
28
29
30

31 **Abstract**

32 Soil erosion hazard is one of the prominent climate hazards that negatively impact countries'
33 economies and livelihood. According to the global climate index, Sri Lanka is ranked among
34 the first ten countries most threatened by climate change during the last three years (2018-
35 2020). However, limited studies were conducted to simulate the impact of the soil erosion
36 vulnerability based on climate scenarios. This study aims to assess and predict soil erosion
37 susceptibility using climate change projected scenarios: Representative Concentration
38 Pathways (RCP) in the Central Highlands of Sri Lanka. The potential of soil erosion
39 susceptibility was predicted to 2040, depending on climate change scenarios, RCP 2.6 and RCP
40 8.5. Five models: revised universal soil loss (RUSLE), frequency ratio (FR), artificial neural
41 networks (ANN), support vector machine (SVM) and adaptive network-based fuzzy inference
42 system (ANFIS) were selected as widely applied for hazards assessments. Eight geo-
43 environmental factors were selected as inputs to model the soil erosion susceptibility. Results
44 of the five models demonstrate that soil erosion vulnerability (soil erosion rates) will increase
45 4% - 22% compared to the current soil erosion rate (2020). The predictions indicate average
46 soil erosion will increase to 10.50 t/ha/yr and 12.4 t/ha/yr under the RCP 2.6 and RCP 8.5
47 climate scenario in 2040, respectively. The ANFIS and SVM model predictions showed the
48 highest accuracy (89%) on soil erosion susceptibility for this study area. The soil erosion
49 susceptibility maps provide a good understanding of future soil erosion vulnerability (spatial
50 distribution) and can be utilized to develop climate resilience.

51 **Keywords:** Soil erosion susceptibility; GIS; Adaptive Neuro-Fuzzy Interface; Climate change
52 scenarios; Sri Lanka

53

54 **1. Introduction**

55 Every year, a considerable number of natural disasters take place all over the world. Many
56 countries have suffered from extreme weather events due to the impacts of climate change
57 (Aryal et al., 2020). The global climate risk index indicates to what extent countries and regions
58 have been affected by extreme climate events (floods, cyclones, heat waves etc.). The global
59 climate index shows that Sri Lanka was ranked third, second, and sixth from 2018 to 2020,
60 consecutively (Eckstein et al., 2019). Heavy rainfall, floods, droughts, and many landslide
61 incidents were common in Sri Lanka (Alahacoon et al., 2018; Senanayake et al., 2020).
62 Increasing rainfall and changes in rainfall patterns have been apparent during the past few

63 decades (Nisansala et al., 2020). Due to these climate impacts, the country lost a substantial
64 part of its productive land and millions of dollars in revenues.

65 The Intergovernmental Panel on Climate Change (IPCC) has reported, the global mean
66 precipitation and the surface temperature have changed significantly during the past few
67 decades and will continue to the next century (IPCC, 2015). The warming climates increase
68 the frequency and extent of climate hazards such as droughts and floods. The IPCC's fifth
69 assessment report (AR5) has focused on four future warming scenarios (RCP2.6, RCP4.6,
70 RCP6 and RCP8.5), known as the Representative Concentration Pathway (RCP) scenarios.
71 These scenarios predict how the climate might change from the present to 2100 and beyond.
72 Based on the RCP climate projection, researchers are predicting environmental hazards to take
73 mitigation actions to minimize future emissions (Chen et al., 2020; Magnan et al., 2021).

74 Many researchers have discussed the impacts of climate variation on water erosion (Nearing et
75 al., 2005; Borrelli et al., 2020). However, early researchers mostly neglected climate scenario-
76 based predictions on soil erosion (Mullan et al., 2012). Soil erosion hazard is one of the adverse
77 events due to present climate variation that negatively impacts the environment, agricultural
78 productivity, global food insecurity and livelihoods (Pandey et al. 2016; Lal 2014). Hence,
79 investigating the impacts of climate variation on soil erosion hazards and predicting soil erosion
80 vulnerability is important to introduce mitigating measures to protect precious natural
81 resources. Identification of vulnerable hotspots is also a necessity to implement conservation
82 strategies as well as to direct policy advice. Thereby, modelling the future potential rate of soil
83 erosion is crucial to minimize the adverse impacts from climate variation.

84 Soil erosion prediction models have been employed to quantify and predict the risk of soil
85 erosion (Karydas et al., 2014; Teng et al., 2018). Most of the traditional soil erosion risk
86 assessment methods, such as the physical-based models, have used an exorbitant amount of
87 data as well as the enormous computational cost involved (Teng et al., 2018; Gholami et al.,
88 2021). Soil erosion assessment in large-scale field measurements may cause some
89 disadvantages as cost wise, expensive, time-consuming, and nearly impossible due to limited
90 resources (Batista et al., 2019; Gholami et al., 2021). In addition, soil erosion assessment is
91 highly complex due to the various parameters are involved, and their interactions are highly
92 non-linear (Pandey et al., 2016). Geo-informatics is useful for studying events bearing multi-
93 dimensional behaviours, such as soil erosion, when considering modelling spatial and temporal
94 aspects on the ground (Senanayake et al., 2020).

95 In the recent past, soft computing techniques have been widely applied in many fields, such as
96 floods, drought and gully erosion (Janizadeh et al., 2021). Machine learning (ML) algorithms
97 have been used to model complex non-linear datasets for accurate prediction. These models
98 can identify complex changes or unpredictable situations. ML algorithms learn skills and
99 continue to develop accuracy and performance(Luo et al., 2021). ML algorithms can analyze
100 vast quantities of data, well suited for resolving multi-dimensional and multi-variety
101 information. Most importantly, these models have performed well in a data scarcity
102 environment. Chu et al. (2010) revealed that ML has better efficiency than other models when
103 examining the impact of runoff due to climate change. Soil erosion hazards such as gully
104 erosions were assessed using ML and deep learning models, such as an artificial neuron
105 network (ANN), Support Vector Machine (SVM) and convolution neural network (CNN) (S.
106 Saha et al., 2021), Boosted Tree (BT), Extreme Gradient Boosting (XGB), and Deep Boost
107 (DB) (Chen et al., 2021)in recent years.

108 ML models have been frequently used by combining traditional-based models (Olden et al.,
109 2008). ML modelling methods, such as ANN, SVM, and field data, have been used for soil
110 erosion assessments (Gholami et al., 2021). Gholami et al. (2021) employed erosion pins and
111 ANN to evaluate the spatial distribution of annual soil erosion rates. Combining soil erosion
112 pins with an ANN-based model and obtaining GIS-based outputs was reliable (RMSE:0.1;
113 R^2 :0.9), low-cost, and easy-to-use approach for estimating the annual soil erosion. Zhang et al.
114 (2009) performed soil erosion assessment using the Soil and Water Assessment Tool (SWAT),
115 a physical-based soil erosion model with ANN and SVM models for soil erosion prediction.
116 They found SVM model predicts better with approximating the SWAT model. A fuzzy
117 interface system (FIS) has been widely used for time series prediction in uncertain
118 situations. ANFIS is a hybrid method of ANN and FIS, which can execute the advantages of
119 both these methods.

120 Modelling soil erosion for current and future climate scenarios is crucial for reducing potential
121 environmental hazards and maintaining sustainable land resources (Panagos et al., 2021).
122 Continuous observation and predictions are essential to detect vulnerability for soil erosion in
123 climate variation (Li and Fang, 2016; Mullan et al., 2012). A proper understanding of the
124 locations and magnitude of erosion for present and future situations is required to achieve the
125 UN Sustainable Development Goals (SDGs) (Lal et al., 2021). However, limited knowledge is
126 on soil erosion predictions over the climate scenarios. Hence, this study aims to develop a

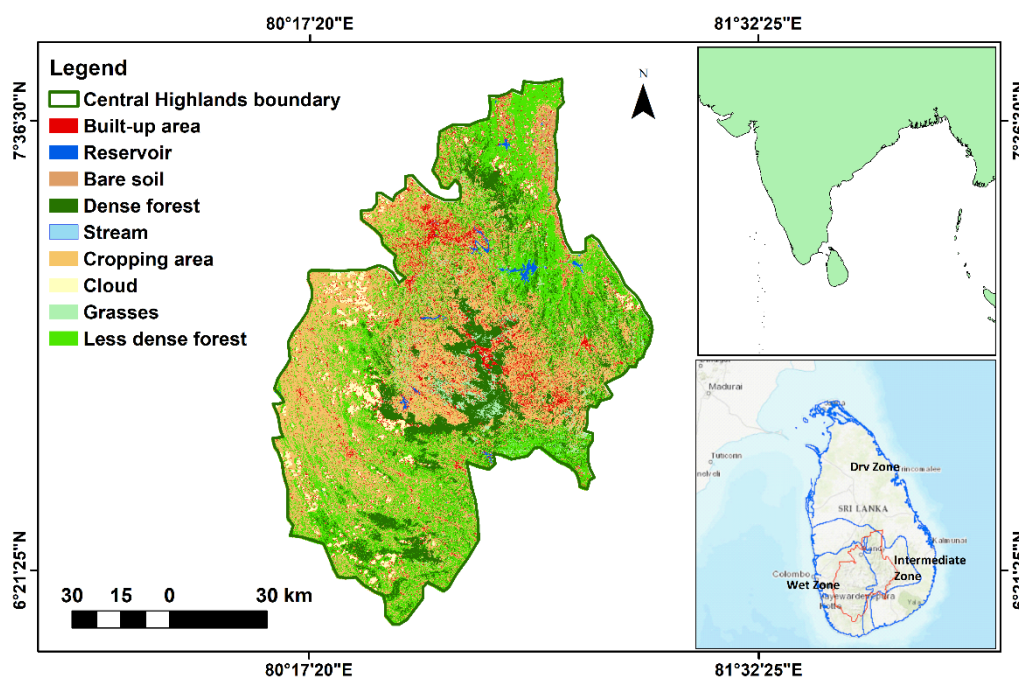
127 spatiotemporal process to predict soil erosion vulnerability using climate scenarios. This
 128 research employed five different models: empirical soil erosion model (RUSLE), statistical
 129 (FR), machine learning (ANN, SVM) and hybrid methods (ANFIS) to explore an accurate
 130 predicting model to find the vulnerability for soil erosion under two different climate scenarios.
 131 This research provides a novel approach by employing five different models and climate
 132 change scenarios using geoinformation tools. In addition, this research investigated the
 133 variation of satellite data and compared it with actual ground data. As per the authors' best of
 134 knowledge, no one has predicted the soil erosion susceptibility for the Sri Lankan context using
 135 climate scenarios. Therefore, the originality of this research is to predict soil erosion hazards
 136 vulnerability using RCP scenarios for the Central Highlands to minimize the impacts of climate
 137 change.

138

139 2. Materials and Method

140 2.1 Study area and data sets

141 The Central Highlands of Sri Lanka is located within 6° 12' to 7° 42' N latitudes and 80° 10' to
 142 81° 15' E longitudes (Figure 1), the maximum and minimum elevations of 300m and 2565 m
 143 a.s.l., with an area of about 10,500 km². The natural landscape of the highlands mainly receives
 144 rainfall from two monsoons and two inter-monsoons. The average rainfall is above 2500 mm
 145 for the western side, and the eastern side receives above 1500mm throughout the year.



146

147

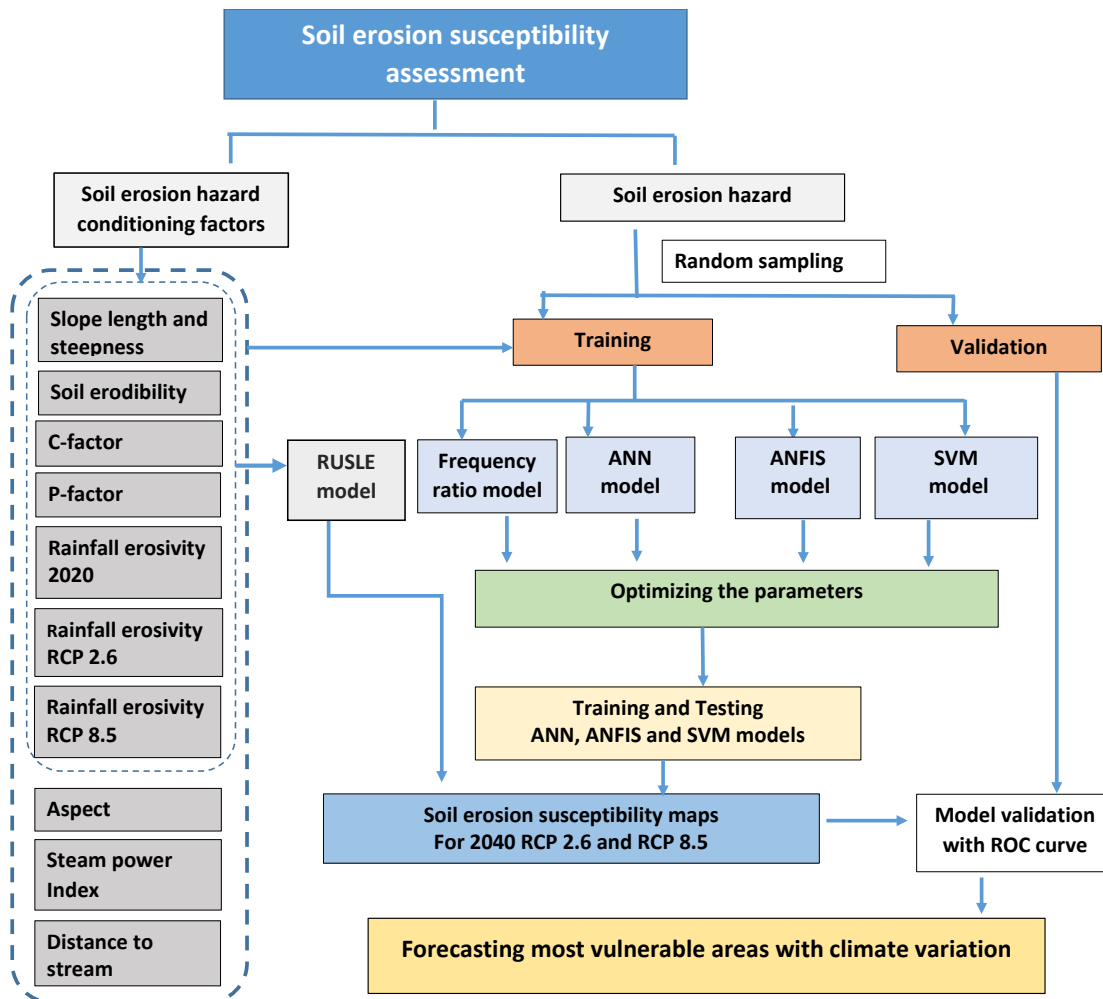
Figure 1. Location of the Study area: the Central Highlands of Sri Lanka.

148 **Table 1.** Summary of the data sources.

Data	Resolution	Source
Soil data	30m	Natural Resources Management Center (NRMC), Sri Lanka
Precipitation data from 1990 to 2019	30m	NRMC, Sri Lanka https://www.doa.gov.lk/NRMC/index.php/en/
Topographic data	30m	Survey Department of Sri Lanka
Past landslides incidences		UNISDR (United Nations International Strategy for Disaster Reduction) http://www.desinventar.lk:8081/DesInventar/index.jsp
Landsat images	30m	USGS earth explore https://earthexplorer.usgs.gov
Climate System Model (CCSM) projections		https://gisclimatechange.ucar.edu/inspector
National Center for Atmospheric Research (NCAR)		http://www.worldclim.org/

149

150 This study developed a spatiotemporal process to project the soil erosion vulnerability with
 151 future climate scenarios. This research employed a combined methodology by using: empirical
 152 soil erosion models, statistical, machine learning, and hybrid methods and techniques for
 153 modelling and projecting soil erosion under two different RCP climate scenarios. The study
 154 deployed a novel approach using five different models together for the projection of the soil
 155 erosion hazards using geoinformatics techniques and evaluating the best model performance
 156 for the projection. The overall methodology is illustrated in Figure 2.



157

158

Figure 2. The overall workflow of the study.

159 **2.2 Soil erosion susceptibility mapping using RUSLE**

160 The soil erosion vulnerability over the Central Highlands was derived from using the RUSLE.
 161 The RUSLE model (Renard et al., 1997) has been commonly employed to estimate long-term
 162 soil erosion rates in agricultural watersheds, regional or country-level, in large-scale studies
 163 (Panagos and Katsoyiannis 2019; Panagos et al. 2015). Many researchers employed the RUSLE
 164 model to predict soil erosion (Teng et al., 2018; Panagos et al., 2021). Accordingly, the RUSLE
 165 model was employed in this study to assess and predict the average annual soil loss of the
 166 Central Highlands for 2020 and 2040 using the following equation (1):

167

$$168 \quad A = R \times K \times L \times S \times C \times P \quad (1)$$

169 The average annual rate of soil erosion (A) is provided in tons per hectare per year. The past
 170 30 years of gauge rainfall data (1990-2019) and 20 years of satellite rainfall data from NCAR
 171 were collected to estimate the rainfall erosivity (R) factor ($\text{MJ mm ha}^{-1} \text{ h}^{-1} \text{ yr}^{-1}$). The RCP

172 scenarios were developed based on statistically downscaled 1-degree precipitation data for
173 2040. The soil erodibility (K) factor ($t\ ha^{-1}\ MJ^{-1}mm^{-1}$), slope length and steepness (LS) factor
174 (unitless), crop factor (C) (unitless) and management practices (P) factor (unitless) were
175 executed from the data gathered from (Senanayake et al., 2020). Detail explanation of the
176 analysis is given in (Senanayake et al., 2020).

177 Soil erosion in the Central Highlands was mainly driven by precipitation. The predicted rainfall
178 raster layers for 2040 (R factors) with other erosion factors (K, LS, C, and P) were used to
179 generate the vulnerability maps. The LS, R, K, C, and P-factor layers were generated in the
180 GIS environment. These layers were multiplied using the raster calculator. The generated soil
181 erosion vulnerability maps were classified into five classes according to the previous
182 classifications of Senanayake et al. (2020).

183 **2.3 Soil erosion susceptibility using frequency ratio**

184 The frequency ratio (FR) model is a statistical-based bivariate approach, which can be
185 employed to detect the spatial relationship among independent and dependent variables. This
186 FR method has been employed to analyze the possibility of an event occurrence using
187 probability mapping by Bonham-Carte (1994). FR can be computed using equation 2.

$$188 \quad FR = \frac{N_{(LS_i)}/N_{(A_i)}}{\sum N_{(LS_i)}/\sum N_{(A_i)}} \quad (2)$$

189
190 where, $N_{(LS_i)}$ is the number of hazard events in class (i), $N_{(A_i)}$ is the total number of pixels in
191 class (i). When the FR value is 1, an average possibility for occurrence, a value higher than 1,
192 means a higher probability of occurrence, and a value lower than one means a low probability
193 of hazard events (Senanayake et al., 2020).

194 **2.3.1 Soil erosion hotspots**

195 Landslides are one of the major natural disasters happening every year in the Central
196 Highlands. A large amount of soil is delivered to streams due to landslides (Gunatilaka, 2007).
197 The amount of sediments delivered to the reservoirs and tributaries is remarkably increased in
198 recent years. Researchers highlighted it might be much larger than the flows of sediments
199 supplied by other erosion processes.

200 Researchers have obtained more reliable soil erosion susceptibility results by introducing
201 landslides incidents. The soil erosion conditioning factors have been used in landslide
202 susceptibility prediction (Huang et al., 2020). Researchers found a correlation between soil
203 erosion and landslide occurrences in several locations (Rozos et al., 2013). Although rainfall
204 plays a leading role in landslide susceptibility in Sri Lanka, researchers found soil erosion may
205 also contribute as one of the reasons for these incidences (Senanayake et al., 2020). Therefore,
206 past landslides incidences were used as training and testing datasets. The locations of 279 soil
207 erosion hot spots were selected, of which 70% and 30% were randomly divided for training
208 and validation purposes. A total of 279 landslides locations (initiated during 2000 - 2019) were
209 recorded from UNISDR (2021).

210 **2.3.2 Soil erosion conditioning factors**

211 The selection of suitable soil erosion conditioning factors is one of the prerequisites for soil
212 erosion assessment and mapping. In the present study, the selection of the most suitable
213 conditioning factors was drawn based on extensive literature reviews and expert advice. Soil
214 erosion susceptibility was analyzed using eight conditioning factors, including rainfall
215 erosivity under two climate scenarios RCP 2.6 for best and RCP 8.5 for the worst situation.
216 Following soil erosion conditioning factors were used: soil erodibility, slope length and
217 steepness, rainfall erosivity, land cover, aspect, distance to stream and steam power Index. The
218 condition factors are explained in detail in the supplementary note S2 sections.

219 **2.3.3 The variable importance**

220 The variable importance (VI) was calculated to evaluate the importance of the soil erosion
221 conditioning factors. The VI was calculated by using SPSS 27 package, according to the study
222 of Termeh et al. (2018). The variable importance value is bounded by 0 and 1. The relative
223 importance of each factor was obtained.

224 **2.4 Artificial neural network methods**

225 ANN has been applied for non-linear complex environmental applications. ANN is ML model
226 that constructs soil erosion causative factors as inputs, and soil erosion can observe using
227 output. The most popularized ANN model for prediction is multilayered perceptron (MLP).
228 MLP with a three-layered interconnected neural network was performed using soil erosion
229 causative factors as input notes. The weightage computations of the input data were used for

230 hidden layer activation, and identity function was used for output layer activation. The weight
231 component act as a coefficient to the inputs. The hidden layer computed the output through a
232 non-linear activation function. The trial-and-error method was performed to determine the
233 number of neurons for the hidden layer. The poor or excessive number of neurons in the hidden
234 layers most likely cause the problems of bad generalization and overfitting (Orhan et al., 2011).
235 A detailed explanation of the ANN model simulation was given in supplementary note S4.

236 **2.5 The adaptive neuro-fuzzy inference system**

237 The adaptive neuro-fuzzy inference system (ANFIS) is employed as a hybrid method by a
238 combination of the fuzzy inference system and the ANN method. This method was developed
239 by Jang (1993) using the Takagi–Sugeno rule format. This hybrid-learning algorithm is a
240 combination of gradient descent and the least square method. ANFIS is a process of fuzzy logic
241 and artificial neural network methods used to drive the fuzzy If-then rules into the artificial
242 neural network with high computational power. Fuzzy rules are implemented along with
243 suitable membership functions of training paired and further lead to an interface. The best
244 possible combination of input parameters provides the best results with the highest accuracy
245 (Islam et al., 2018). The main purpose of employing ANFIS prediction model is due to its rapid
246 learning ability, automatic adaptation capability and capturing nonlinearity of a complex
247 process such as soil erosion (Islam et al., 2018). Figure S2 shows the ANFIS architecture
248 developed by this study.

249 **2.6 Support vector machine algorithm**

250 Support vector machine (SVM) is one of the most popular ML algorithms and is considered a
251 high-performing technique. The SVM algorithm is a non-parametric supervised classification
252 technique introduced by Vapnik proposed in 1995 (Cortes and Vapnik, 1995). Researchers
253 revealed SVM is on statistical learning theory based on the principles of structural risk
254 minimization. A detailed explanation of the SVM model simulation was given in
255 supplementary note S3.

256 The ANN, ANFIS and SVM models were constructed using soil erosion conditioning factors
257 as input. The resulting FR values were used as observed output or dependent variables using
258 MATLAB software. The optimum value for each model was obtained from the trial-and-error

259 method. Conditioning factor raster map layers (30m) were developed (Figure S1) using natural
260 breaks. The soil erosion susceptibility maps were developed in GIS software.

261
262 **2.7 The model validation using a statistical method**

263 The models' performances were evaluated using mean-absolute-error (MAE) and root-mean-
264 square-error (RMSE). Validation of soil erosion risk maps was done using ROC/AUC analysis.
265 The ROC curve was obtained using SPSS software for the validation of soil erosion
266 susceptibility maps. The AUC value is equal to 1 indicates the perfect model prediction. The
267 ROC curves were established based on the false positive rate (1-specificity) and the true
268 positive rate (sensitivity) with the various cutoff thresholds.

269
$$\text{RMSE} = \sqrt{\frac{\sum_{i=1}^N [\bar{X} - X]^2}{N}} \quad (8)$$

270
$$\text{MAE} = \frac{1}{N} \sum_{i=1}^N [\bar{X} - X] \quad (9)$$

271 where N is the sample size, \bar{X} indicates predicted values, and X is observed values. Means
272 absolute error is the sum of the deviation between predicted values of a variable and the real
273 observed values. RMSE optimal value is zero (0), which indicates a higher model performance
274 and prediction rate. However, the optimal value is close to zero is relative. Hence, previous
275 studies revealed that RMSE with standard deviation (SD) of the observation values is
276 appropriate for evaluating the acceptable model performance (Singh et al., 2005; Moriasi et al.,
277 2007; Kastridis et al., 2020).

278
279 **3. Results**

280 **3.1 Soil erosion susceptibility mapping and model performance**

281 Predictions show average soil erosion rates will increase to 10.5 t/ha/yr under the RCP 2.6 and
282 12.4 t/ha/yr under the RCP 8.5 climate scenario in 2040. The results of RUSLE indicate the
283 soil erosion rate in 2020 is 10.18 t/ha/yr with the satellite rainfall data. However, the ground-
284 based gauge rainfall data indicate soil erosion rate is much higher than the results of satellite
285 rainfall data (11.8 t/ha/yr). The average annual rainfall variation over the past 20 years derived
286 from gauge and satellite data are illustrated in Figure 3.

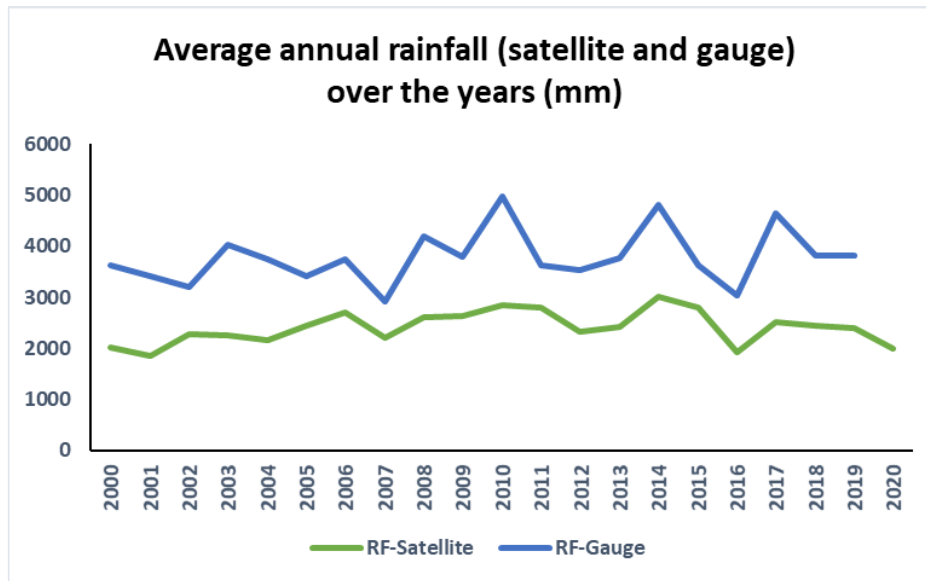


Figure 3: Average annual rainfall in Rathnapura area

287

288

289 The areas covered by soil erosion hazards high and very-high categories are increasing in 2040,
 290 with a projected RCP 8.5 scenario. The risk of soil erosion vulnerability in RCP 8.5 is greater
 291 than RCP 2.5. The respective soil erosion susceptibility maps and the area covered by each soil
 292 erosion category are illustrated in Figure S6 and Table 2.

293 **Table 2.** Area covered by the soil erosion category from the RUSLE model.

Class	Soil erosion rate	2020		2040	
		Gauge rainfall	Satellite rainfall	RCP2.6	RCP 8.5
Very Low	<5	5147.04	5228.71	5176.9	4845.05
Low	5-'10	1594.27	1630.48	1604.85	1396.54
Moderate	10 -' 20	1913.96	1927.82	1928.87	1961.01
High	20-50	1463.26	1383.80	1436.95	1765.93
Very High	50<	381.47	329.19	352.42	531.46
Area (km ²)		10500.00	10500.00	10500.00	10500.00

294

295 3.2 Frequency ratio method

296 Soil erosion susceptibility was analyzed with eight conditioning factors using the FR method
 297 (Figure S1). The results of the FR analysis and weight for each factor were given in Table S1.
 298 The soil erodibility, stream power index and slope length and steepness are obtained highest
 299 weights. The susceptibility maps of the frequency ratio method indicate the western side of the
 300 Central Highlands is more vulnerable to the projected RCP 8.5 scenario.

301 3.3 Artificial neural networks method

302 Figure 4 shows the results of the best validation performance curve. The results show that the
 303 best validation performance was achieved from seven epochs, the MSE = 1.31 and R values
 304 for training= 0.95, testing 0.84, validation = 0.85 and overall = 0.91. The best validation
 305 performance curve of the ANN model is given in Figure S5. The resulted weights are given in
 306 Table S3.

307

308

309

310

311

312

313

314

315

316

317

318

319

320

321

322

323

324

325

326

327

328

329

330

331

332

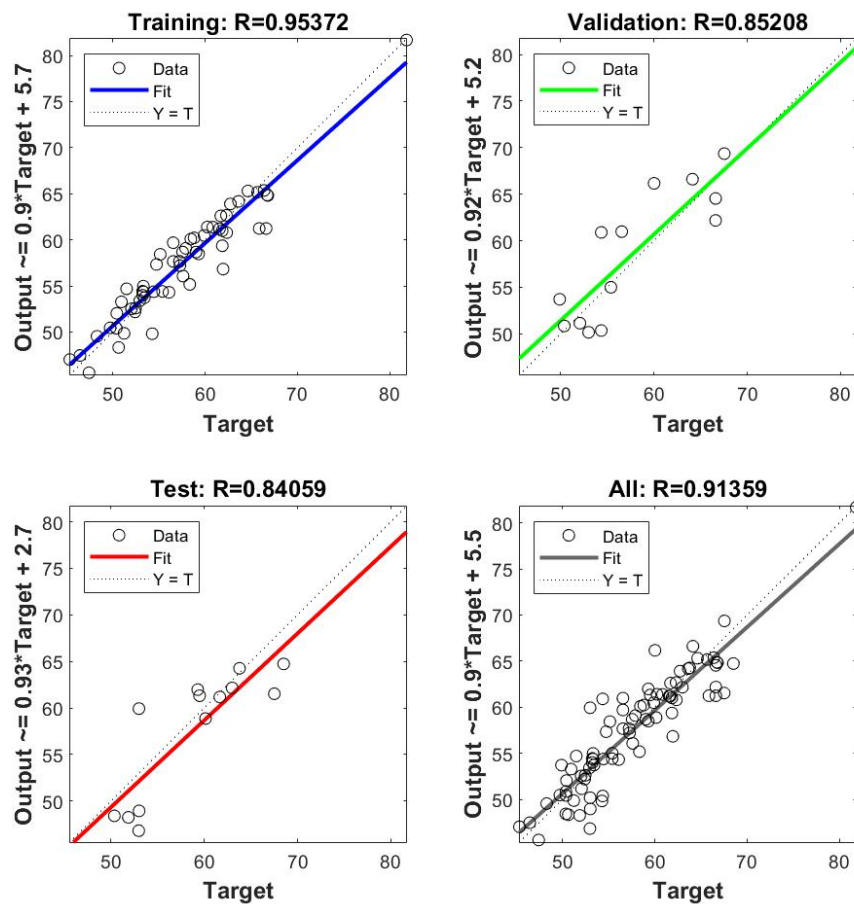


Figure 4. The performance curve of the ANN method.

3.4 Support vector machine learning method

327 This research employed SVM with eight predictors using Gaussian kernel function with
 328 optimization. The performance of SVM is RMSE = 2.29, SD = 4.2 and $R^2= 0.70$. The AUC
 329 indicates soil erosion susceptibility map from the SVM method was performed better than the
 330 ANN model (Figure 7). The RMSE value is 2.29, almost half of SD (4.2), indicating an
 331 acceptable model performance.

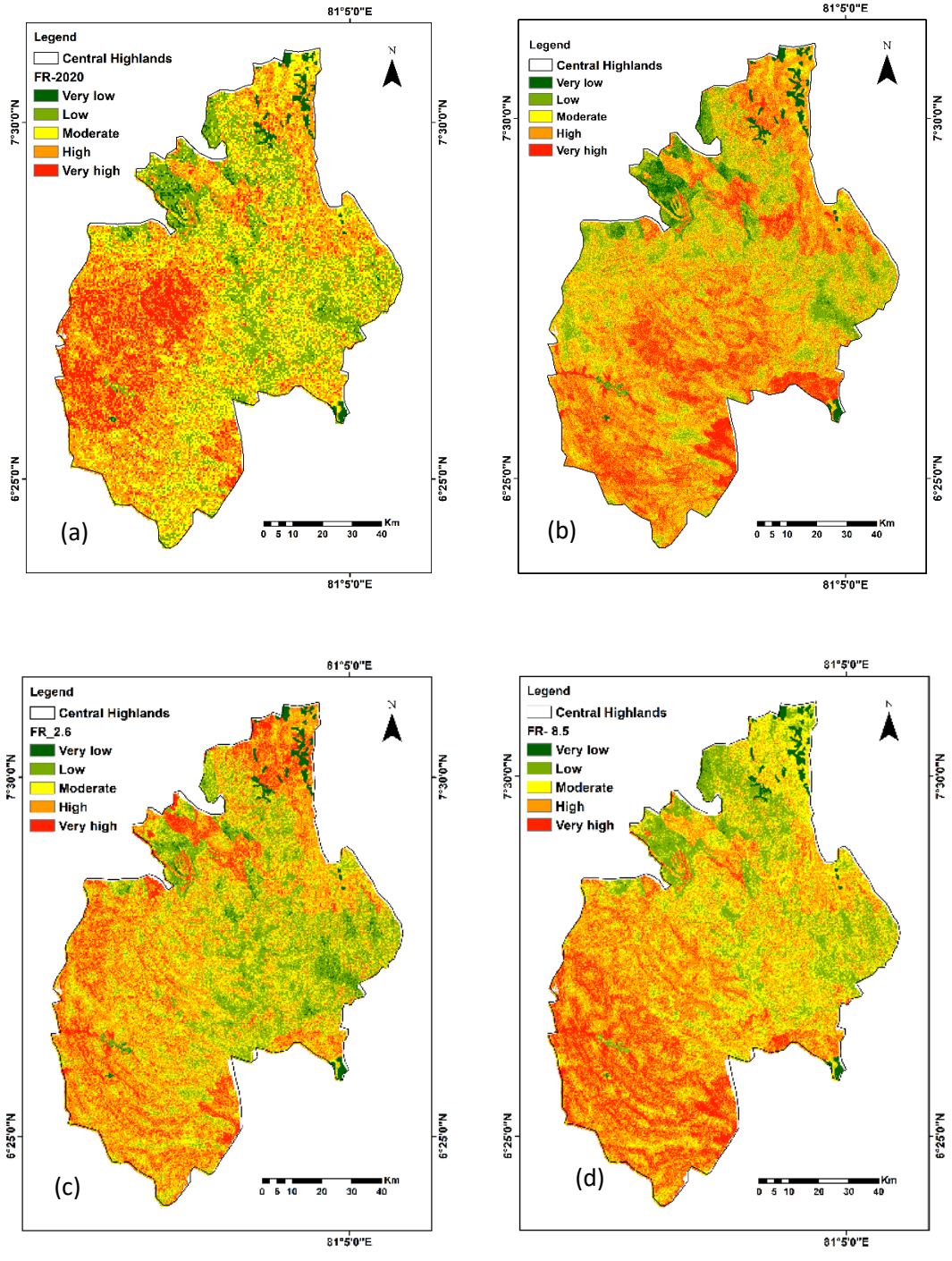
333 **3.5 Adaptive neuro-fuzzy inference system method**

334 The ANFIS model was applied in a trial-and-error method to obtain the best outputs in the
 335 training process. The best validation performance of the ANFIS model was obtained in RMSE
 336 = 0.001 from 2 epochs and $R^2 = 0.73$. The AUC results show ANFIS model performs better
 337 than the ANN model (Figure 7). Figure S8 illustrates a comparison of the ANFIS outcome
 338 and RUSLE outcome. The respective soil erosion susceptibility maps and the area covered by
 339 each soil erosion category are shown in Figure 5 and Table 3.

340 **Table 3.** Area covered by the soil erosion category from the ANFIS model.

Soil erosion Class	2020		2040	
	Gauge RF	Satellite RF	RCP 2.6	RCP-8.5
Very low	282.76	44.65	527.06	45.8
Low	1572.75	1835.24	1671.09	1658.6
Moderate	2719.98	1724.49	1605.08	1560.0
High	4116.70	3870.92	3772.82	3744.5
Very high	1807.81	3024.70	2923.95	3491.1
Area (km ²)	10500.00	10500.00	10500.00	10500.00

341



342

343

344 **Figure 5.** Soil erosion susceptibility map for (a) 2020 from gauged data, (b) 2020 from
 345 satellite data, (c) RCP 2.6, and (d) RCP 8.5 in 2040.

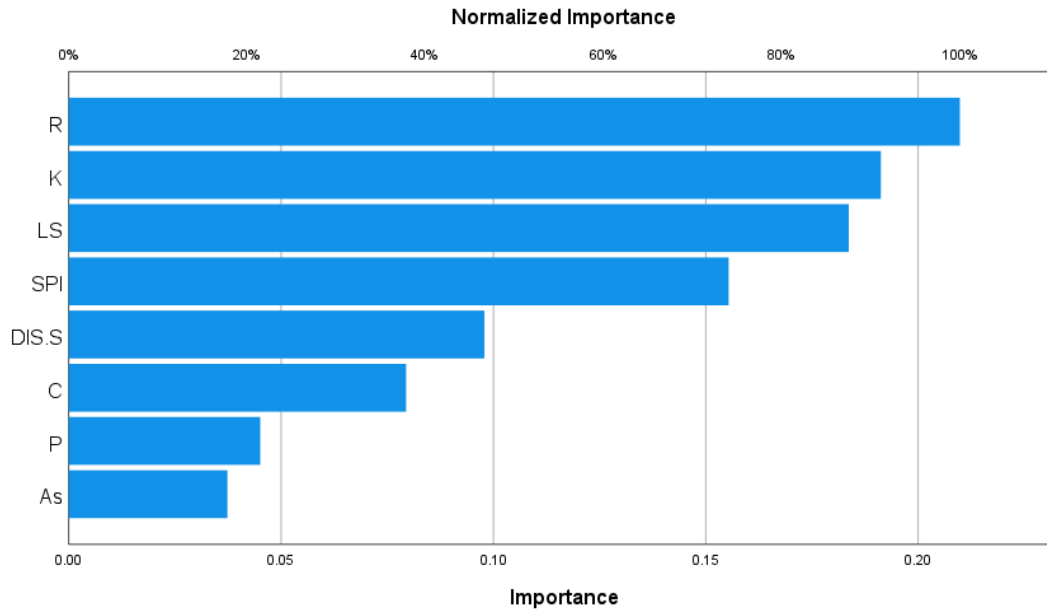
346

347

348

349 **3.6 Relative importance of the soil erosion conditioning factors**

350 The variable importance calculation method results indicate that rainfall, soil erodibility, slope
 351 length, and steepness are the most responsible factors for soil erosion susceptibility in this study
 352 area. Figure 6 illustrates the relative importance of soil erosion conditioning factors.



353 **Figure 6.** The relative importance of soil erosion conditioning factors.
 354

355 **3.7 Validation of susceptibility maps**

356 Figure 7 and Table 4 indicate the model efficiency obtained from ROC and AUC analysis.
 357 Findings of the analyses revealed all five models employed in this study met the requirement
 358 of a threshold value of the ROC curve. The highest AUC values were obtained for ANFIS and
 359 SVM models. The ANN and FR methods received the lowest accuracy levels. A summary of
 360 the models AUC values shows in Table 4.

361 **Table 4.** The model performance using AUC

Test Result Variable(s)	Area under the curve	Std. Error ^a	Asymptotic Sig. ^b	Asymptotic 95% Confidence Interval	
				Lower Bound	Upper Bound
ANFIS_2020	.891	.089	.194	.716	1.000
ANFIS_RCP2.6	.957	.049	.129	.860	1.000
ANFIS_RCP8.5	.891	.102	.219	.670	1.000
SVM-SE2020	.891	.089	.194	.716	1.000
SVM-RCP2.6	.891	.089	.194	.716	1.000

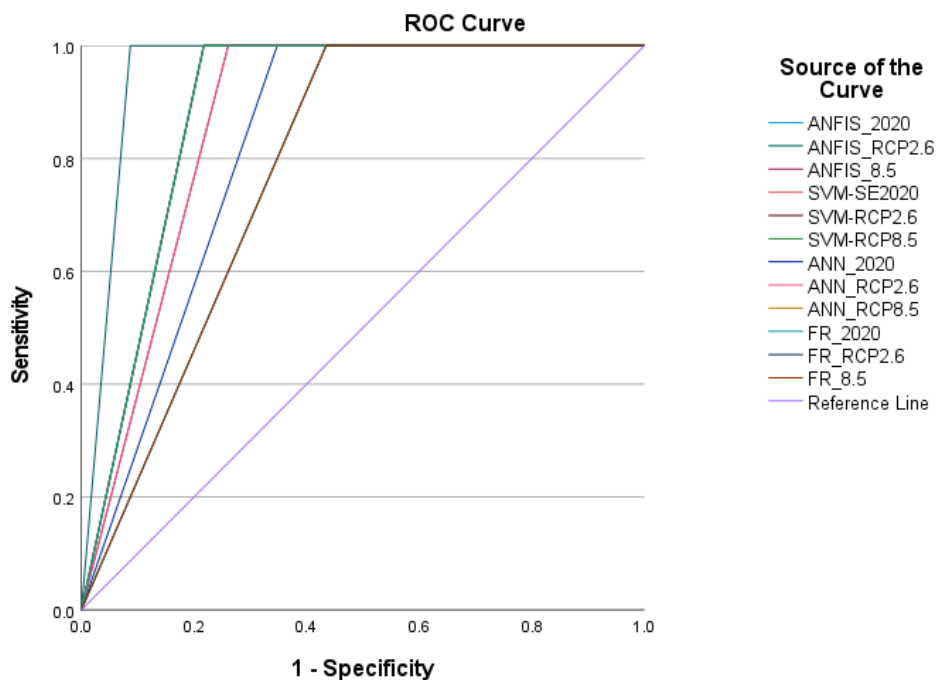
SVM-RCP8.5	.891	.089	.194	.716	1.000
ANN_2020	.826	.126	.279	.579	1.000
ANN_RCP2.6	.870	.102	.219	.670	1.000
ANN_RCP8.5	.891	.089	.194	.716	1.000
FR_2020	.870	.089	.194	.716	1.000
FR_RCP2.6	.783	.150	.348	.489	1.000
FR_RCP8.5	.783	.150	.348	.489	1.000

a. Under the non-parametric assumption

b. Null hypothesis: true area = 0.5

362

363



364 **Figure 7.** Model validation from ROC curve.

365

366 **4.0 Discussion**

367 The present study contributes by addressing a knowledge gap on a methodological approach
 368 for the spatiotemporal process to predict soil erosion susceptibility in the Central Highlands of
 369 Sri Lanka under different climate scenarios. In addition, this study introduces a methodological
 370 improvement by combining projected rainfall erosivity under RCP scenarios as conditioning
 371 factors for empirical equation, statistical, machine learning and hybrid machine learning
 372 techniques to predict soil erosion. This study suggests that SVM and ANFIS models accurately
 373 predict soil erosion vulnerability at two different climate scenarios.

374 This study identified that soil erosion rates will increase from 4% to 22% in 2040, compared
375 to 2020, under the predicted climate scenarios. The results revealed the current soil erosion rate
376 is 11.8 t/ha/yr (2020) in the Central Highlands. The satellite-based rainfall erosivity shows a
377 relatively low value than gauged rainfall erosivity. That is primarily due to the low spatial
378 resolution of the satellite images. However, satellite and gauge rainfall data have a better
379 correlation ($r=0.62$, KEG's $=0.41$). Researchers have identified that tolerable soil erosion loss
380 is around 1-2 t/ha/yr in the Central Highlands of Sri Lanka (Somasiri et al., 2021). According
381 to the projected RCP8.5 scenario, all models employed in this study indicate soil erosion
382 susceptibility and vulnerability are increasing. In other words, the risk of soil erosion will be
383 high, specifically in western parts of the Central Highlands, by 2040. Although the areas
384 covered by different soil erosion susceptibility classes are varied, one thing is prominent. The
385 areas covered by very high and high susceptibility classes under projected RCP 8.5 are
386 increasing in 2040 with all the models (Figure S7).

387 The above findings are in line with the study of Zheng et al. (2018). This estimated future
388 climate and runoff projections across South Asia, including Sri Lanka, using a consistent
389 method by 42 General circulation models (GCMs) in CMIP5. The modelling results indicate
390 that projected runoff will increase throughout the region. The change of runoff is occurred due
391 to the changes in precipitation. The median projection indicates the mean annual runoff
392 increases by 20–30% in the Indian sub-continent by 2046–2075 relative to 1976–2005.

393 Researchers found that increasing rainfalls influence the soil erosion runoff in the western
394 slopes of the Central Highlands. They have observed rainfall variation in terms of increasing
395 rainfall intensity and average rainfall. Burt and Weerasinghe (2014) had investigated the main
396 drivers of changes in daily precipitation in Sri Lanka. They found sea surface temperature of
397 the Pacific and Indian ocean drives the atmospheric changes of regional climate change.
398 Researchers observed that increasing one degree of Celsius in the global mean temperature
399 increases water holding capacity in the atmosphere by 7%, resulting in intense rainfall and a
400 vigorous hydrological cycle (Mullan et al., 2012). This study also identified rainfall and soil
401 erodibility are the most important factors for soil erosion hazards in this study area. Hence, the
402 areas with steep slopes and higher altitudes are more vulnerable to climate variability.
403 Specifically western part of the Central Highlands will be more susceptible to soil erosion.

404 It is important to understand the risk of soil erosion in terms of physical, transitional, and human
405 risk and their possible consequences for better preparedness. A recent study found that high

406 intensive rainfall caused sudden and long-travelling landslides in the Central Highlands of Sri
407 Lanka (Dang et al., 2019). Within three consecutive days, the above area received 446.5 mm
408 heavy rainfall from May 14 to 17, 2017. Soil mass movement caused more significant damage
409 in the Aranayake area by killing 127 people and demolishing 75 houses. In addition, almost all
410 the houses in this area are still at risk of future landslides. Perera et al. (2018) have observed
411 that 52% of household incomes were generated from agricultural activities, home-garden and
412 plantation agriculture. The landslide has badly affected the social and economic aspects of the
413 household, as well as the country's economy. This implies the possible risk of soil erosion
414 hazards, which will enhance landslide incidences and damage to agricultural activities and
415 livelihoods. It will also be threatening the lives of peoples and may possibility of peoples'
416 migration to other areas. Hence, the potential risk of future environmental problems is
417 important to reduce the negative consequences.

418 Hewawasam and Illangasinghe (2015) have identified the rate of soil erosion in the Central
419 Highlands that significantly reduce the reservoirs' capacity. They have identified the major
420 rivers and their tributaries transport a heavy load of sediments during the rainy seasons, which
421 is a severe threat to the storage capacity of reservoirs that supply water for hydropower
422 generation and agricultural production in the country. However, Diyabalanage et al. (2017)
423 have researched to identify the impact of soil and water conservation measures on soil erosion
424 rate and sediment yield. They have identified with this mitigation measures a five-fold
425 reduction in the sediment load of the streams in the critical areas that successfully contributed
426 to soil erosion reduction. Therefore, considerable attention should be paid to strengthening soil
427 conservation measures over the highlands. The potential risk of soil erosion and changing
428 rainfall patterns should be further studied.

429 Soil erodibility mainly depends on the chemical and physical structure of the soil (De Rouw
430 and Rajot, 2004). The Central Highlands is covered by 73% of Red-Yellow Podzolic soils
431 which have relatively high soil erodibility value. Increasingly, lands are exposed to poor
432 agricultural practices, resulting in poor soil organic matter content. That implies a loss of soil
433 structure (chemical and physical) and subsequently less stable aggregates (De Rouw and Rajot,
434 2004). Researchers found the agricultural land areas are increasing from 2000 to 2019 in the
435 Central Highlands with increasing soil erosion rates (Senanayake et al., 2020). This indicates
436 more attention should be paid to improving the soil condition by taking appropriate measures,
437 such as increasing the organic matter content, especially in highly vulnerable areas for soil

438 erosion. In addition, this research proposes to conduct research on soil erodibility assessment
439 under different land uses. The results will indicate the critical soil organic matter content values
440 in different land uses.

441 The findings of this study contribute to resilience development for future agricultural planning
442 and management. Soil erosion susceptibility maps with the vulnerability assessment can be
443 useful for land managers and policymakers with respect to agricultural strategic planning and
444 environmental protection. Quantifying the impacts of climate variability and its effects on soil
445 erosion over the study area is important to assist the land managers in adopting new techniques
446 and conservation strategies to protect and minimize further damages or prevent the occurrence
447 of disasters such as landslides. This research proposes further education and awareness
448 programs on soil erosion and conservation strategies (Lal et al., 2021), integrated agro-
449 meteorological advisory services, adaptation measures for climate resilience agriculture, social
450 networking and community-based adaptation as long term - strategies for resilience
451 development on soil conservation (Aryal et al., 2020). The projected increasing rainfall and
452 runoff subsequently influence increasing runoff and gully erosion. Hence, improving the
453 drainage system to remove excess water from the land may need to protect the soil from runoff.
454 In addition, the construction of rain-shelters such as protected agriculture technology/
455 polytunnel may need to protect crops from intense or erratic rainfall.

456 The limitation of this study is socio-economic factors were not incorporated into this analysis.
457 However, these factors may influence soil erosion over the next century. These projections
458 could be achieved when the mitigation targets of RCPs are combined with the Shared
459 Socioeconomic Pathways (SSPs) in the Coupled in Model Intercomparison Project Phase 6
460 (CMIP6). The SSP scenarios look at five different ways the world might evolve in the absence
461 of climate policy or how different levels of climate change need mitigation. These projections
462 include socio-economic factors such as population, economic growth, education, urbanization
463 and the rate of technological development. Almazroui et al. (2020) researched the latest CMIP6
464 dataset to examine the projected changes in temperature and precipitation over six South Asian
465 countries. The average annual precipitation is projected to increase by 25.1% in Sri Lanka
466 under the SSP5-8.5 scenario by the end of the twenty-first century. The projected temperature
467 increases by 1.2 °C, 2.1 °C, and 4.3 °C under the SSP1-2.6, SSP2-4.5, and SSP5-8.5 scenarios,
468 respectively, over South Asia.

469 Lal et al. (2021) emphasized that sustainable soil management is key to achieving the SDGs.
470 They have highlighted achieving SDGs: 2-zero hunger, 3-good health and well-being, 6- clean
471 water and sanitation, 13- climate action, 15 - life on land and 17- partnership have a direct
472 connection with the soil activities. This research contributes to addressing some of the decision-
473 making challenges to achieve the SDGs in the 2030 UN agenda, such as identifying appropriate
474 methods for risk assessment, understanding the location and magnitude of erosion, forecasting
475 changes in soil erosion driven by water, land use, and climate change. Healthy soils maintain
476 the eco-service activities in the farming systems and improve food security in a country.

477 **5. Conclusion**

478 The study focuses on five models: RUSLE, FR, ANN, SVM, and ANFIS, to predict and
479 quantify soil erosion vulnerability in the Central Highlands of Sri Lanka. Soil erosion
480 susceptibility was analyzed using eight conditioning factors to observe the soil erosion
481 vulnerability for the present situation and 2040 under projected RCP 2.6 and RCP 8.5 climate
482 scenarios. The results suggest the soil erosion rate in 2040 will increase to 10.5 t/ha/yr and 12.4
483 t/ha/y under RCP 2.6 and RCP 8.5, respectively, which increase the recommended threshold
484 value in the country and tolerable soil loss value globally (10 t/ha/y). The frequency ratio
485 method is the least accurate model for predicting soil erosion vulnerability. The probability
486 maps of the ANFIS and SVM methods provide the highest accurate model predictions
487 (accuracy 89%). The rainfall and soil erodibility are the most influential factors for hazards
488 vulnerability. The results of these models' outputs indicate farming systems in the western
489 slopes of the Central Highlands will be more vulnerable to soil erosion hazards under climate
490 scenario RCP 8.5 in 2040. Findings suggest implementing soil conservation activities with
491 short-and long-term strategies help to achieve the SGDs in the UN agenda 2030.

492 **Funding:** The research is funded by the Centre for Advanced Modeling and Geospatial
493 Information Systems (CAMGIS), Faculty of Engineering & IT, University of Technology
494 Sydney.

495 **Author Contributions:** Conceptualization, S.S. and B.P.; methodology, S.S., B.P.; formal
496 analysis, S.S.; validation, S.S.; writing- original draft preparation, S.S.; writing - review and
497 editing, S.S., B.P., supervision, B.P., funding acquisition, B.P.

498 **Declaration of Competing Interest:** The authors declare that they have no known competing
499 financial interests or personal relationships that could have appeared to influence the work
500 reported in this paper.

501 **Reference**

- 502 Alahacoon, N., Matheswaran, K., Pani, P., Amarnath, G., 2018. A decadal historical satellite
503 data and rainfall trend analysis (2001-2016) for flood hazard mapping in Sri Lanka.
504 *Remote Sens.* 10, 448. <https://doi.org/10.3390/rs10030448>
- 505 Almazroui, M., Saeed, S., Saeed, F., Islam, M.N., Ismail, M., 2020. Projections of Precipitation
506 and Temperature over the South Asian Countries in CMIP6. *Earth Syst. Environ.* 4, 297–
507 320. <https://doi.org/10.1007/s41748-020-00157-7>
- 508 Aryal, J.P., Sapkota, T.B., Khurana, R., Khatri-Chhetri, A., Rahut, D.B., Jat, M.L., 2020.
509 Climate change and agriculture in South Asia: adaptation options in smallholder
510 production systems. *Environ. Dev. Sustain.* 22, 5045–5075.
511 <https://doi.org/10.1007/s10668-019-00414-4>
- 512 Batista, P.V.G., Davies, J., Silva, M.L.N., Quinton, J.N., 2019. On the evaluation of soil erosion
513 models: Are we doing enough? *Earth-Science Rev.*
514 <https://doi.org/10.1016/j.earscirev.2019.102898>
- 515 Bonham-Carte, G., 1994. Computer methods in the geosciences, in: *Geographic Information*
516 *Systems for Geoscientists*. Elsevier, p. ii. [https://doi.org/10.1016/b978-0-08-041867-](https://doi.org/10.1016/b978-0-08-041867-4.50001-1)
517 [4.50001-1](https://doi.org/10.1016/b978-0-08-041867-4.50001-1)
- 518 Borrelli, P., Robinson, D.A., Panagos, P., Lugato, E., Yang, J.E., Alewell, C., Wuepper, D.,
519 Montanarella, L., Ballabio, C., 2020. Land use and climate change impacts on global soil
520 erosion by water (2015-2070). *Proc. Natl. Acad. Sci. U. S. A.* 117, 21994–22001.
521 <https://doi.org/10.1073/pnas.2001403117>
- 522 Burt, T.P., Weerasinghe, K.D.N., 2014. Rainfall distributions in Sri Lanka in time and space:
523 An analysis based on daily rainfall data. *Climate* 2, 242–263.
524 <https://doi.org/10.3390/cli2040242>
- 525 Chen, W., Lei, X., Chakraborty, R., Chandra Pal, S., Sahana, M., Janizadeh, S., 2021.
526 Evaluation of different boosting ensemble machine learning models and novel deep
527 learning and boosting framework for head-cut gully erosion susceptibility. *J. Environ.*
528 *Manage.* 284, 112015. <https://doi.org/10.1016/j.jenvman.2021.112015>
- 529 Chen, Y., Liu, A., Cheng, X., 2020. Quantifying economic impacts of climate change under
530 nine future emission scenarios within CMIP6. *Sci. Total Environ.* 703, 134950.
531 <https://doi.org/10.1016/j.scitotenv.2019.134950>
- 532 Chu, J.T., Xia, J., Xu, C.Y., Singh, V.P., 2010. Statistical downscaling of daily mean
533 temperature, pan evaporation and precipitation for climate change scenarios in Haihe
534 River, China. *Theor. Appl. Climatol.* 99, 149–161. [https://doi.org/10.1007/s00704-009-](https://doi.org/10.1007/s00704-009-0129-6)
535 [0129-6](https://doi.org/10.1007/s00704-009-0129-6)
- 536 Cortes, C., Vapnik, V., 1995. Support-vector networks. *Mach. Learn.* 20, 273–297.
537 <https://doi.org/10.1007/bf00994018>
- 538 Dang, K., Sassa, K., Konagai, K., Karunawardena, A., Bandara, R.M.S., Hirota, K., Tan, Q.,
539 Ha, N.D., 2019. Recent rainfall-induced rapid and long-traveling landslide on 17 May
540 2016 in Aranayaka, Kagelle District, Sri Lanka. *Landslides* 16, 155–164.
541 <https://doi.org/10.1007/s10346-018-1089-7>
- 542 De Rouw, A., Rajot, J.L., 2004. Soil organic matter, surface crusting and erosion in Sahelian

543 farming systems based on manuring or fallowing, in: *Agriculture, Ecosystems and*
544 *Environment*. pp. 263–276. <https://doi.org/10.1016/j.agee.2003.12.020>

545 Diyabalanage, S., Samarakoon, K.K., Adikari, S.B., Hewawasam, T., 2017. Impact of soil and
546 water conservation measures on soil erosion rate and sediment yields in a tropical
547 watershed in the Central Highlands of Sri Lanka. *Appl. Geogr.* 79, 103–114.
548 <https://doi.org/10.1016/j.apgeog.2016.12.004>

549 Eckstein, D., Wingses, M., Marie-Lena, H., 2019. Global climate risk index 2019 [WWW
550 Document]. URL <https://germanwatch.org/en/16046> (accessed 5.8.21).

551 Gholami, V., Sahour, H., Hadian, A., Mohammad, A., 2021. Soil erosion modeling using
552 erosion pins and artificial neural networks. *Catena* 196, 104902.
553 <https://doi.org/10.1016/j.catena.2020.104902>

554 Gunatilaka, A., 2007. Role of basin-wide landslides in the formation of extensive alluvial
555 gemstone deposits in Sri Lanka. *Earth Surf. Process. Landforms* 32, 1863–1873.
556 <https://doi.org/10.1002/esp.1498>

557 Hewawasam, T., Illangasinghe, S., 2015. Quantifying sheet erosion in agricultural highlands
558 of Sri Lanka by tracking grain-size distributions. *Anthropocene* 11, 25–34.
559 <https://doi.org/10.1016/j.ancene.2015.11.004>

560 Huang, F., Chen, J., Du, Z., Yao, C., Huang, J., Jiang, Q., Chang, Z., Li, S., 2020. Landslide
561 susceptibility prediction considering regional soil erosion based on machine-learning
562 models. *ISPRS Int. J. Geo-Information* 9. <https://doi.org/10.3390/ijgi9060377>

563 IPCC, 2015. AR5 Synthesis Report (LONG) Climate Change 2014 1–167.

564 Islam, M.R., Jaafar, W.Z.W., Hin, L.S., Osman, N., Hossain, A., Mohd, N.S., 2018.
565 Development of an intelligent system based on ANFIS model for predicting soil erosion.
566 *Environ. Earth Sci.* 77, 186. <https://doi.org/10.1007/s12665-018-7348-z>

567 Jang, J.S.R., 1993. ANFIS: Adaptive-Network-Based Fuzzy Inference System. *IEEE Trans.*
568 *Syst. Man Cybern.* 23, 665–685. <https://doi.org/10.1109/21.256541>

569 Janizadeh, S., Chandra Pal, S., Saha, A., Chowdhuri, I., Ahmadi, K., Mirzaei, S., Mosavi, A.H.,
570 Tiefenbacher, J.P., 2021. Mapping the spatial and temporal variability of flood hazard
571 affected by climate and land-use changes in the future. *J. Environ. Manage.* 298, 113551.
572 <https://doi.org/10.1016/j.jenvman.2021.113551>

573 Jayawardena, I.M.S.P., Darshika, D.W.T.T., C. Herath, H.M.R., 2018. Recent Trends in
574 Climate Extreme Indices over Sri Lanka. *Am. J. Clim. Chang.* 07, 586–599.
575 <https://doi.org/10.4236/ajcc.2018.74036>

576 Karydas, C.G., Panagos, P., Gitas, I.Z., 2014. A classification of water erosion models
577 according to their geospatial characteristics. *Int. J. Digit. Earth* 7, 229–250.
578 <https://doi.org/10.1080/17538947.2012.671380>

579 Kastridis, A., Kirkenidis, C., Sapountzis, M., 2020. An integrated approach of flash flood
580 analysis in ungauged Mediterranean watersheds using post-flood surveys and unmanned
581 aerial vehicles. *Hydrol. Process.* 34, 4920–4939. <https://doi.org/10.1002/hyp.13913>

582 Lal, R., 2014. Climate Strategic Soil Management. *Challenges* 5, 43–74.
583 <https://doi.org/10.3390/challe5010043>

- 584 Lal, R., Bouma, J., Brevik, E., Dawson, L., Field, D.J., Glaser, B., Hatano, R., Hartemink, A.E.,
585 Kosaki, T., Lascelles, B., Monger, C., Muggler, C., Ndzana, G.M., Norra, S., Pan, X.,
586 Paradelo, R., Reyes-Sánchez, L.B., Sandén, T., Singh, B.R., Spiegel, H., Yanai, J., Zhang,
587 J., 2021. Soils and sustainable development goals of the United Nations: An International
588 Union of Soil Sciences perspective. *Geoderma Reg.*
589 <https://doi.org/10.1016/j.geodrs.2021.e00398>
- 590 Li, Z., Fang, H., 2016. Impacts of climate change on water erosion: A review. *Earth-Science*
591 *Rev.* <https://doi.org/10.1016/j.earscirev.2016.10.004>
- 592 Luo, D., Caldas, M.M., Goodin, D.G., 2021. Estimating environmental vulnerability in the
593 cerrado with machine learning and Twitter data. *J. Environ. Manage.* 289, 112502.
594 <https://doi.org/10.1016/j.jenvman.2021.112502>
- 595 Magnan, A.K., Pörtner, H.-O., Duvat, V.K.E., Garschagen, M., Guinder, V.A., Zommers, Z.,
596 Hoegh-Guldberg, O., Gattuso, J.-P., 2021. Estimating the global risk of anthropogenic
597 climate change. *Nat. Clim. Chang.* 11, 879–885. [https://doi.org/10.1038/s41558-021-](https://doi.org/10.1038/s41558-021-01156-w)
598 [01156-w](https://doi.org/10.1038/s41558-021-01156-w)
- 599 Moriasi, D.N., Arnold, J.G., Van Liew, M.W., Bingner, R.L., Harmel, R.D., Veith, T.L., 2007.
600 Model evaluation guidelines for systematic quantification of accuracy in watershed
601 simulations. *Trans. ASABE* 50, 885–900.
- 602 Mullan, D., Favis-Mortlock, D., Fealy, R., 2012. Addressing key limitations associated with
603 modelling soil erosion under the impacts of future climate change. *Agric. For. Meteorol.*
604 156, 18–30. <https://doi.org/10.1016/j.agrformet.2011.12.004>
- 605 Nearing, M.A., Jetten, V., Baffaut, C., Cerdan, O., Couturier, A., Hernandez, M., Le
606 Bissonnais, Y., Nichols, M.H., Nunes, J.P., Renschler, C.S., Souchère, V., Van Oost, K.,
607 2005. Modeling response of soil erosion and runoff to changes in precipitation and cover,
608 in: *Catena*. Elsevier, pp. 131–154. <https://doi.org/10.1016/j.catena.2005.03.007>
- 609 Nisansala, W.D.S., Abeysingha, N.S., Islam, A., Bandara, A.M.K.R., 2020. Recent rainfall
610 trend over Sri Lanka (1987–2017). *Int. J. Climatol.* 40, 3417–3435.
611 <https://doi.org/10.1002/joc.6405>
- 612 Olden, J.D., Lawler, J.J., Poff, N.L., 2008. Machine learning methods without tears: A primer
613 for ecologists. *Q. Rev. Biol.* <https://doi.org/10.1086/587826>
- 614 Orhan, U., Hekim, M., Ozer, M., 2011. EEG signals classification using the K-means clustering
615 and a multilayer perceptron neural network model. *Expert Syst. Appl.* 38, 13475–13481.
616 <https://doi.org/10.1016/j.eswa.2011.04.149>
- 617 Panagos, P., Ballabio, C., Himics, M., Scarpa, S., Matthews, F., Bogonos, M., Poesen, J.,
618 Borrelli, P., 2021. Projections of soil loss by water erosion in Europe by 2050. *Environ.*
619 *Sci. Policy* 124, 380–392. <https://doi.org/10.1016/j.envsci.2021.07.012>
- 620 Panagos, P., Borrelli, P., Poesen, J., Ballabio, C., Lugato, E., Meusburger, K., Montanarella,
621 L., Alewell, C., 2015. The new assessment of soil loss by water erosion in Europe.
622 *Environ. Sci. Policy* 54, 438–447. <https://doi.org/10.1016/j.envsci.2015.08.012>
- 623 Panagos, P., Katsoyiannis, A., 2019. Soil erosion modelling: The new challenges as the result
624 of policy developments in Europe. *Environ. Res.*
625 <https://doi.org/10.1016/j.envres.2019.02.043>
- 626 Pandey, A., Himanshu, S.K., Mishra, S.K., Singh, V.P., 2016. Physically based soil erosion

627 and sediment yield models revisited. *Catena*. <https://doi.org/10.1016/j.catena.2016.08.002>

628 Perera, E.N.C., Jayawardana, D.T., Jayasinghe, P., Bandara, R.M.S., Alahakoon, N., 2018.
629 Direct impacts of landslides on socio-economic systems: a case study from Aranayake,
630 Sri Lanka. *Geoenvironmental Disasters* 5, 1–12. [https://doi.org/10.1186/s40677-018-](https://doi.org/10.1186/s40677-018-0104-6)
631 [0104-6](https://doi.org/10.1186/s40677-018-0104-6)

632 Renard, K.G., Foster, G.R., Weesies, G., McCool, D., Yoder, D., 1997. Predicting soil erosion
633 by water: a guide to conservation planning with the Revised Universal Soil Loss Equation
634 (RUSLE). *Agric. Handb. No. 703*. <https://doi.org/DC0-16-048938-5> 65–100.

635 Rozos, D., Skilodimou, H.D., Loupasakis, C., Bathrellos, G.D., 2013. Application of the
636 revised universal soil loss equation model on landslide prevention. An example from N.
637 Euboea (Evia) Island, Greece. *Environ. Earth Sci.* 70, 3255–3266.
638 <https://doi.org/10.1007/s12665-013-2390-3>

639 Saha, S., Sarkar, R., Thapa, G., Roy, J., 2021. Modeling gully erosion susceptibility in
640 Phuentsholing, Bhutan using deep learning and basic machine learning algorithms.
641 *Environ. Earth Sci.* 80, 295. <https://doi.org/10.1007/s12665-021-09599-2>

642 Senanayake, S., Pradhan, B., Huete, A., Brennan, J., 2020. Assessing Soil Erosion Hazards
643 Using Land-Use Change and Landslide Frequency Ratio Method: A Case Study of
644 Sabaragamuwa Province, Sri Lanka. *Remote Sens.* 12, 1483.
645 <https://doi.org/10.3390/rs12091483>

646 Singh, J., Knapp, H.V., Arnold, J.G., Demissie, M., 2005. Hydrological modeling of the
647 Iroquois River watershed using HSPF and SWAT. *J. Am. Water Resour. Assoc.* 41, 343–
648 360. <https://doi.org/10.1111/j.1752-1688.2005.tb03740.x>

649 Somasiri, I.S., Hewawasam, T., Rambukkange, M.P., 2021. Adaptation of the revised universal
650 soil loss equation to map spatial distribution of soil erosion in tropical watersheds: a
651 GIS/RS-based study of the Upper Mahaweli River Catchment of Sri Lanka. *Model. Earth*
652 *Syst. Environ.* 1, 3. <https://doi.org/10.1007/s40808-021-01245-x>

653 Teng, H., Liang, Z., Chen, S., Liu, Y., Viscarra Rossel, R.A., Chappell, A., Yu, W., Shi, Z.,
654 2018. Current and future assessments of soil erosion by water on the Tibetan Plateau based
655 on RUSLE and CMIP5 climate models. *Sci. Total Environ.* 635, 673–686.
656 <https://doi.org/10.1016/j.scitotenv.2018.04.146>

657 Termeh, S.V.R., Kornejady, A., Pourghasemi, H.R., Keesstra, S., 2018. Flood susceptibility
658 mapping using novel ensembles of adaptive neuro fuzzy inference system and
659 metaheuristic algorithms. *Sci. Total Environ.* 615, 438–451.
660 <https://doi.org/10.1016/j.scitotenv.2017.09.262>

661 UNISDR, 2021. Inventar [WWW Document]. *Desaster Inf. Syst.* URL
662 <http://www.desinventar.lk:8081/DesInventar/> (accessed 5.14.21).

663 Zhang, X., Srinivasan, R., Van Liew, M., 2009. Approximating SWAT model using artificial
664 neural network and support vector machine. *J. Am. Water Resour. Assoc.* 45, 460–474.
665 <https://doi.org/10.1111/j.1752-1688.2009.00302.x>

666 Zheng, H., Chiew, F.H.S., Charles, S., Podger, G., 2018. Future climate and runoff projections
667 across South Asia from CMIP5 global climate models and hydrological modelling. *J.*
668 *Hydrol. Reg. Stud.* 18, 92–109. <https://doi.org/10.1016/j.ejrh.2018.06.004>

669